Available online at www.sciencedirect.com

SciVerse ScienceDirect

Advances in Space Research 52 (2013) 375–382

ADVANCES IN SPACE RESEARCH (a COSPAR publication)

www.elsevier.com/locate/asr

Modeling and observations of the north–south ionospheric asymmetry at low latitudes at long deep solar minimum

N. Balan [a,*], P.K. Rajesh [a], S. Sripathi [b], S. Tulasiram [b], J.Y. Liu [a], G.J. Bailey [c]

[a] Institute of Space Sciences, National Central University, Chung-Li 32054, Taiwan
[b] Indian Institute of Geomagnetism, Mumbai, India
[c] Applied Mathematics, University of Sheffield, Sheffield, UK

Received 25 December 2012; received in revised form 5 April 2013; accepted 6 April 2013
Available online 3 May 2013

Abstract

Using the physics based model SUPIM and FORMOSAT-3/COSMIC electron density data measured at the long deep solar minimum (2008–2010) we investigate the longitude variations of the north–south asymmetry of the ionosphere at low latitudes (±30° magnetic). The data at around diurnal maximum (12:30–13:30 LT) for magnetically quiet (Ap ⩽ 15) equinoctial conditions (March–April and September–October) are presented for three longitude sectors (a) 60°E–120°E, (b) 60°W–120°W and (c) 15°W–75°W. The sectors (a) and (b) have large displacements of the geomagnetic equator from geographic equator but in opposite hemispheres with small magnetic declination angles; and sector (c) has large declination angle with small displacement of the equators; vertical **E** × **B** drift velocities also have differences in the three longitude sectors. SUPIM investigates the importance of the displacement of the equators, magnetic declination angle, and **E** × **B** drift on the north–south asymmetry. The data and model qualitatively agree; and indicate that depending on longitudes both the displacement of the equators and declination angle are important in producing the north–south asymmetry though the displacement of the equators seems most effective. This seems to be because it is the displacement of the equators more than the declination angle that produces large north–south difference in the effective magnetic meridional neutral wind velocity, which is the main cause of the ionospheric asymmetry. For the strong control of the neutral wind, east–west electric field has only a small effect on the longitude variation of the ionospheric asymmetry. Though the study is for the long deep solar minimum the conclusions seem valid for all levels of solar activity since the displacement of the equators and declination angle are independent of solar activity.

Keywords: Ionosphere; North–south asymmetry; Neutral wind; Electric field; Geomagnetic and geographic equators

1. Introduction

The solar minimum between solar cycles 23 and 24 was an unusual minimum lasting over four years in 2006–2010, which dipped to the deepest minimum in 2008 in a century (Russell et al., 2010; Girish & Gopkumar, 2012). The long deep solar minimum provided unique opportunities to investigate the intrinsic properties of the upper atmosphere–ionosphere–plasmasphere system, and its interactions with the regions below with minimum forcing from above. A number of interesting observations has been reported covering the unusual solar minimum (e.g., Heelis et al., 2008; Goncharenko et al., 2010; Luhr and Xiong, 2010; Abdu, 2012; Balan, Chen, Liu, & Bailey, 2012; and references therein). In this paper using the physics based model SUPIM (Sheffield University Plasmasphere Ionosphere Model) (Bailey and Balan, 1996) and the FORMOSAT-3/COSMIC electron density (Ne) data measured at the long deep solar minimum (e.g., Lin et al., 2007; Liu

* Corresponding author. Tel.: +886 3 422715/65775; fax: +886 3 4224394.
E-mail addresses: b.nanan@sheffield.ac.uk (N. Balan), pkrgere@gmail.com (P.K. Rajesh), ssripathi.iig@gmail.com (S. Sripathi), s.tulasiram@gmail.com (S. Tulasiram), tigerjyliu@gmail.com (J.Y. Liu), g.bailey@sheffield.ac.uk (G.J. Bailey).

0273-1177/$36.00
http://dx.doi.org/10.1016/j.asr.2013.04.003

et al., 2010a,b) we investigate the north–south asymmetry of the ionosphere at low latitudes (±30° magnetic). Though observations of the asymmetry at the unusual solar minimum have been presented (e.g., Tulasi Ram et al., 2009), to our knowledge, no modeling of the asymmetry has been reported. Though the study is for the long deep solar minimum the conclusions seem valid for all levels of solar activity.

The ionosphere is expected to be more or less symmetric with respect to the geomagnetic equator at around equinoxes when inter-hemispheric transport of plasma is expected to be a minimum. But observations have shown significant north–south asymmetry at the equinoxes, with the ionosphere being denser in one hemisphere than in the other (e.g., Mehmet, 1988; Balan, Bailey, Moffett, Su, & Titheridge, 1995; Tulasi Ram et al., 2009). Mehmet (1988) studied the asymmetry in peak electron density (Nmax) at magnetically conjugate low latitude stations in African and West Asian regions, and found that daytime Nmax in the northern equatorial ionization anomaly (EIA) crest is greater than that in the southern EIA crest; and at night the asymmetry is reversed. The observed asymmetry is interpreted in terms of the north–south differences in the meridional neutral wind velocity. The north–south asymmetry in total electron content (TEC) at low latitudes during evening-midnight period was reported by Balan et al. (1995).

The COSMIC Ne data have been used to study several aspects of the low-mid latitude ionosphere at the long deep solar minimum (e.g., Lin et al., 2007; Tulasi Ram et al., 2009; Liu et al., 2010a,b; Balan et al., 2012; and references therein). Lin et al. (2007) reported the first observations of the COSMIC Ne data; they showed the evolution of EIA in July–August 2006 and brought out the disappearance of the well known winter anomaly at the long deep solar minimum. In a study of the behavior of EIA using COSMIC Ne data Tulasi Ram et al. (2009) reported that the magnetic declination angle can modulate the north–south structure of EIA at equinoxes. Recently, Zhang et al. (2012) reported the importance of declination angle and zonal neutral wind on the longitude variation of Ne at mid latitudes.

The north–south ionospheric asymmetry at high solar activity has been modeled (e.g., Balan et al., 1995; Balan, Bailey, Abdu, Oyama, & Richards, 1997; Su, Bailey, Oyama, & Balan, 1997). The models indicate that the asymmetry is caused mainly by the north–south differences in the effective magnetic meridional neutral wind velocity

$$U = U_\theta \cos D + U_\varphi \sin D \quad (1)$$

where U_θ (positive southward) and U_φ (positive eastward) are the meridional and zonal wind velocities, and D (positive eastward) is declination angle; and longitude variation of the wind velocity causes the degree of the asymmetry to vary with longitude. The neutral wind produces the asymmetry due to the (1) displacement of geomagnetic and geographic equators and (2) magnetic declination angle.

The relative importance of the causes (1) and (2) can be better understood at longitudes of maximum displacement of the equators with minimum declination angle, and maximum declination angle with minimum displacement of the equators. We selected three longitude sectors (a) 60°E–120°E, (b) 60°W–120°W (or 240°E–300°E), and (c) 15°W–75°W (or 285°E–345°E) (Fig. 1). The sectors (a) and (b) have large displacements of the geomagnetic equator from geographic equator but in opposite directions (up to 7° and −12°) with small magnetic declination angles (−1.20° and −1.87° near the centers); these sectors are therefore best suited to study the opposite neutral wind effects due to the displacement of the equators. Sector (c) has large declination angle (−18.83° near the center) and small displacement of the equators (0° near the center); sector (c) is therefore best suited to study the effect of magnetic declination angle. Also, on either side of the center of sector (c), the displacements are nearly equal and opposite in the sub-longitude sectors (d) 45°W–75°W and (e) 45°W–15°W. The sub-sectors (d) and (e) can therefore be used to check the opposite effect of the displacement of the equators with large and nearly equal declination angles.

The COSMIC Ne data under equinoctial conditions (March–April and September–October) will be shown for the three main longitude sectors (a, b and c) and two sub-longitude sectors (d and e). Model calculations are carried out for the longitudes 75°E, 75°W and 45°W (dots in Fig. 1), which are near the centers of the longitude sectors, and also fall close to the equatorial ionospheric stations in

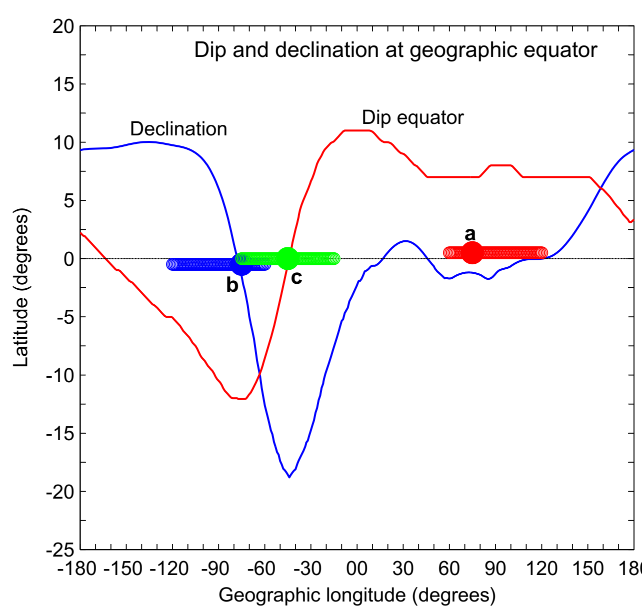

Fig. 1. Latitude of dip equator and magnetic declination angle at geographic equator (in 2010) obtained from IGRF-2011; horizontal bars indicate the longitude bands of interest, with the dots corresponding to the longitudes of modeling.

India (Trivandrum, 8.5°N, 76.9°E; 0.5°S dip angle), Peru (Jicamarca, 11.9°S, 76.9°W; 1.0°N dip angle) and Brazil (Fortaleza, 3.7°S, 38.5°W; 2.0°S dip angle). The purpose of the study is to investigate the importance of the different causes of the north–south asymmetry. However, no data/model comparisons are attempted because measured values of the solar EUV fluxes, and neutral densities and wind velocities are not available.

2. Model and inputs

The physics based model SUPIM (Bailey and Balan, 1996) solves the coupled time-dependent equations of continuity, momentum and energy for the electrons and ions (O^+, H^+, He^+, N_2^+, NO^+, and O_2^+) along closed eccentric-dipole geomagnetic field lines. The modeling procedure is same as that described recently (Balan et al., 2010). The model inputs are the vertical $\mathbf{E} \times \mathbf{B}$ drift velocities at the equator, neutral wind velocities, neutral densities and temperatures, and solar EUV fluxes.

The vertical $\mathbf{E} \times \mathbf{B}$ drift patterns used are the average patterns for the 500–800 km range at March equinox (March–April) in 2009 measured by C/NOFS satellite (Stoneback et al., 2011), which are shown in Fig. 2 (red for 75°E, blue for 75°W and green for 45°W). The drift velocities in the three sectors differ by up to 10 m s^{-1} during daytime; and unlike at normal solar minimum, the drift velocities, in general, undergo semi-diurnal variations with downward reversal in the afternoon (~14 LT) (Stoneback et al., 2011). The drift velocities are applied to all field lines (apex height 150–11,000 km) and hence to all altitudes and latitudes. The possible altitude variation (over the equator) of the $\mathbf{E} \times \mathbf{B}$ drift cannot be incorporated due to the non-availability of the measured velocities at different altitudes over the equator or at different latitudes, though SUPIM has the capability to incorporate the variation (e.g., Bailey and Balan, 1996). The drift velocity varies along the field lines in accordance with the field-line geometry (Bailey and Balan, 1996). Solar EUV fluxes are from the EUV94 model (Tobiska, 1991).

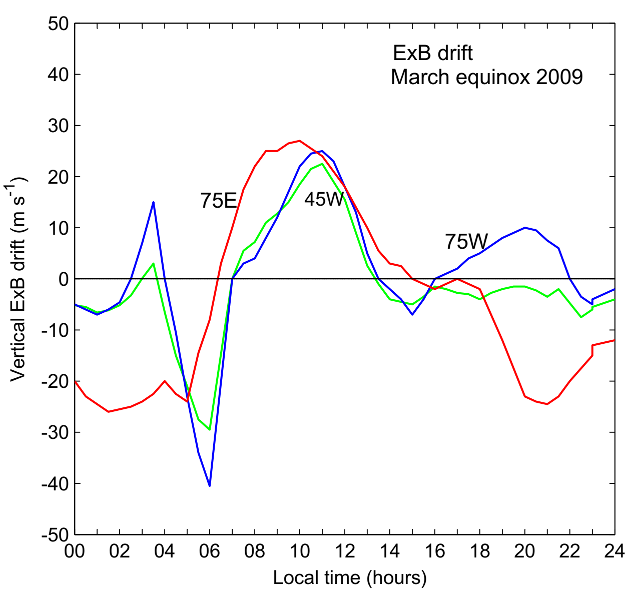

Fig. 2. Local time variations of the vertical $\mathbf{E} \times \mathbf{B}$ drift velocity at March equinox in the three longitude sectors 60°E–120°E (red), 60°W–120°W (blue) and 15°W–75°W (green) at the long deep solar minimum (2009); scaled from Stoneback et al. (2011). (For interpretation of the references to colour in this figure legend, the reader is referred to the web version of this article.)

The neutral wind velocities are from HWM91 (Hedin et al., 1991), and neutral densities and temperatures are from MSIS86 (Hedin, 1987). HWM (horizontal wind model) and MSIS represent the thermosphere reasonably well; and provide values of neutral wind velocities, densities and temperatures as function of altitude, latitude, longitude and local time. SUPIM calculates the effective magnetic meridional wind velocity U (Eq. (1)). Sample local time variations of U at 300 km height at 16°N and 16°S (magnetic latitudes) are shown in Fig. 3 for the longitudes 75°E, 75°W and 45°W (panels a, b, and c). The wind velocities during daytime (11–15 LT) of interest are asymmetric in north and south in all three longitudes. During this local time interval, at 75°E and 75°W the wind flows in opposite

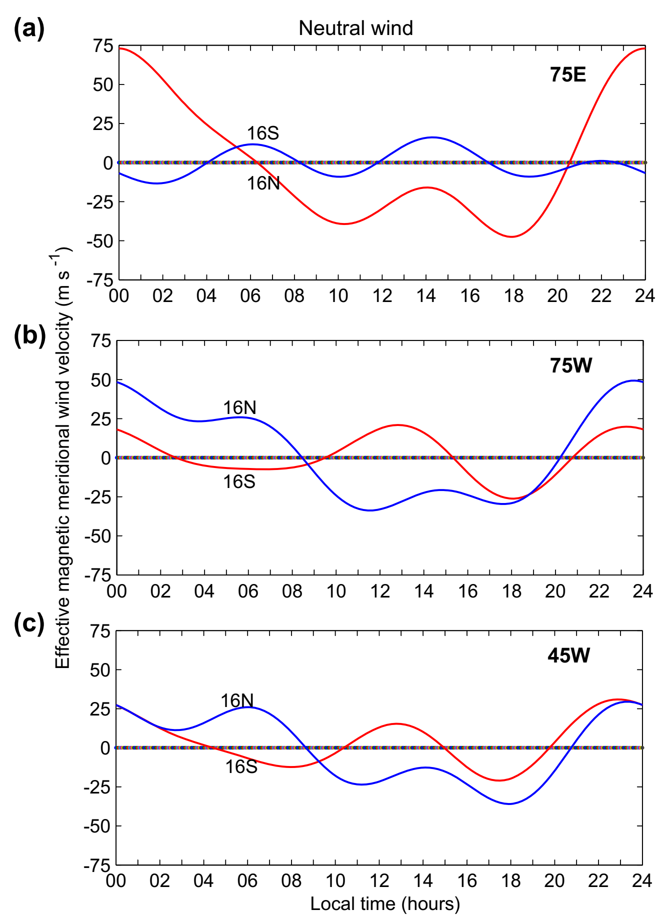

Fig. 3. Sample local time variations of the effective magnetic meridional neutral wind velocity at 300 km height at 16°N and 16°S magnetic latitudes in (a) 75°E, (b) 75°W and (c) 45°W.

directions in both north and south; and at 75°W and 45°W the wind directions are same though the velocities are small at 45°W.

3. Model results

As mentioned above, model calculations are carried out for 75°E, 75°W and 45°W longitudes at the deep solar minimum (F10.7 = 68) under magnetically quite (Ap = 4) March equinox (day number 80) conditions. First the same **E** × **B** drift pattern (corresponding to 75°W, blue, Fig. 2) is used in all three longitudes to model the effects of neutral wind. Then the actual **E** × **B** drifts in the three longitudes are used to model the effects of the drifts.

3.1. Neutral wind effect

Fig. 4 shows the altitude-latitude plots of the model electron density Ne at 13 LT in 75°E (panel a), 75°W (panel b) and 45°W (panel c). To get a better picture of the altitude dependence of the north–south asymmetry, the latitude variations of the electron density Ne at fixed altitudes and peak electron density Nmax (at 13 LT) are shown in Fig. 5 (panels a–c). The corresponding total electron content TEC (integrated up to 1600 km altitude) variations are shown by the solid curves in Fig. 6 (red 75°E, blue 75°W, and green 45°W). As mentioned above, these results are obtained using the same **E** × **B** drift (blue, Fig. 2). The model values of Ne, Nmax and TEC produce the equatorial ionization anomaly (EIA) with trough around the equator, crests at around ±16° magnetic latitudes (in Nmax) and crest-to-trough ratio about 1.5 (in Nmax) in all three longitudes. However, in vertical TEC (Fig. 6) the crests are at lower latitudes and crest-to-trough ratios are smaller than those in Nmax; this is because the EIA crests in Ne (Figs. 4 and 5) shift to lower latitudes with increasing altitudes and disappear at around 600 km.

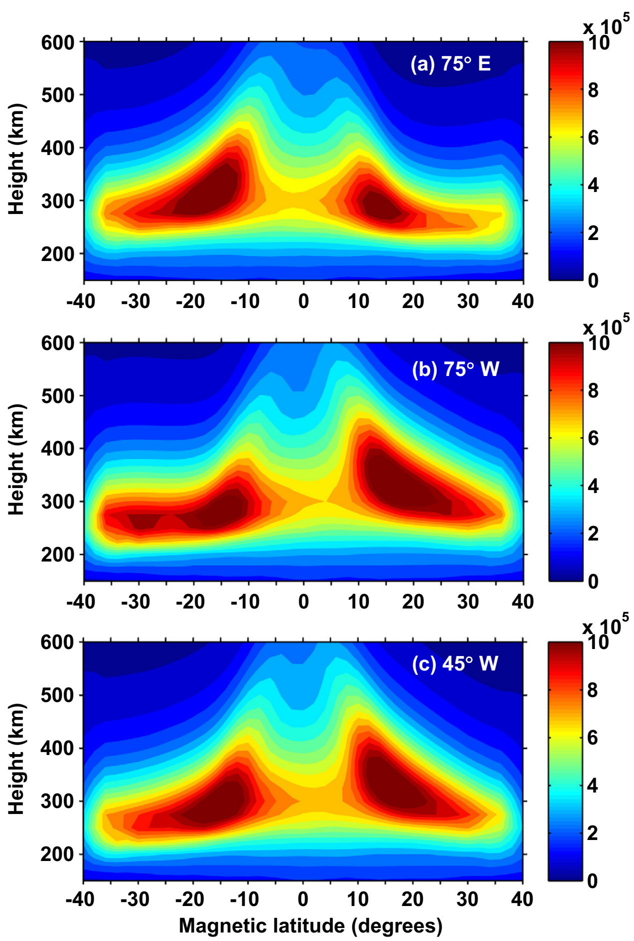

Fig. 4. Altitude-latitude plots of model Ne at 13 LT at March equinox (day 80) for Ap = 4 and F10.7 = 68 in (a) 75°E, (b) 75°W and (c) 45°W obtained using the same vertical **E** × **B** drift velocity (blue, Fig. 2) in all three longitudes; positive latitude is north. (For interpretation of the references to colour in this figure legend, the reader is referred to the web version of this article.)

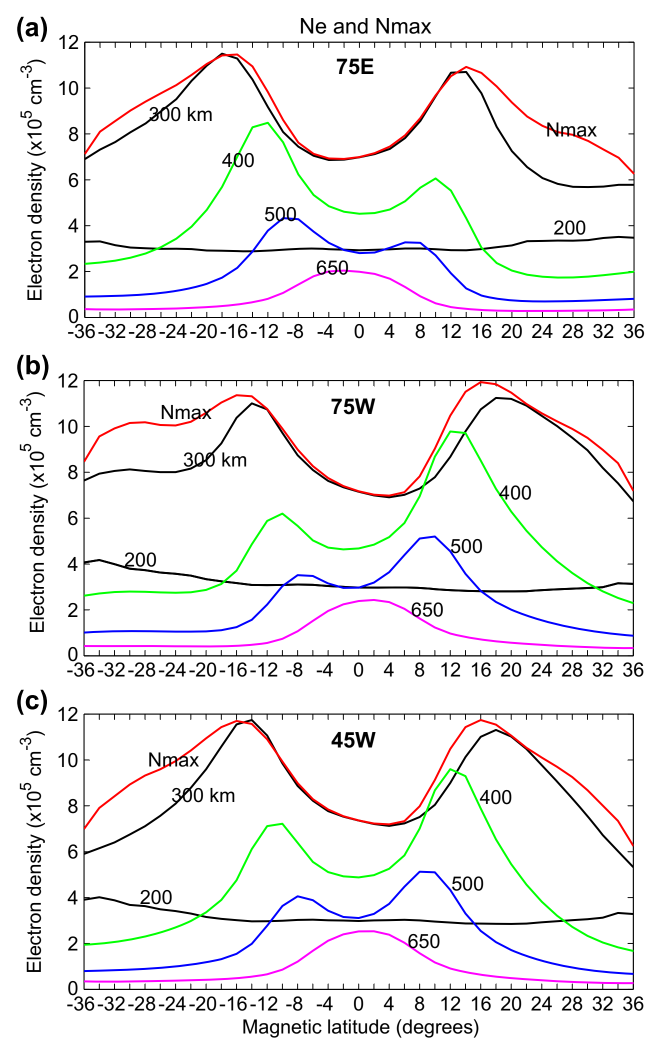

Fig. 5. Latitude variations of model Ne (at 200 km, 300 km, 400 km, 500 km and 650 km) and Nmax at 13 LT at March equinox (day 80) for Ap = 4 and F10.7 = 68 in (a) 75°E, (b) 75°W and (c) 45°W obtained using the same vertical **E** × **B** drift velocity (blue, Fig. 2) in all three longitudes; positive latitude is north. (For interpretation of the references to colour in this figure legend, the reader is referred to the web version of this article.)

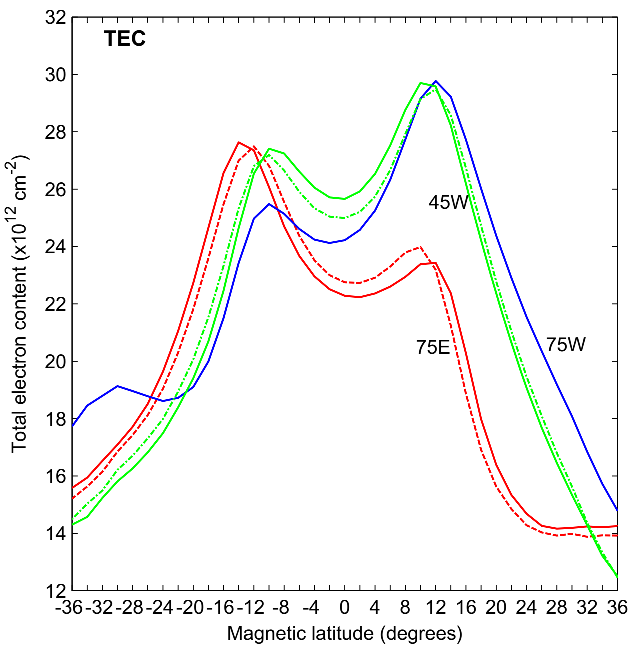

Fig. 6. Latitude variations of model vertical TEC (integrated up to 1600 km) at 13 LT at March equinox (day 80) for Ap = 4 and F10.7 = 68 in 75°E (red), 75°W (blue) and 45°W (green) obtained using same vertical **E** × **B** drift (blue, Fig. 2) in all three longitudes (solid curves). The dashed curves correspond to the TEC obtained using the **E** × **B** drift patterns corresponding to the three longitudes (Fig. 2). Positive latitude is north. (For interpretation of the references to colour in this figure legend, the reader is referred to the web version of this article.)

The model results (Figs. 4–6) also show north–south asymmetry in Ne, Nmax and TEC. However, there is no significant asymmetry in Ne in the chemistry dominated bottomside ionosphere (e.g., 200 km) indicating that thermospheric composition is nearly symmetric in north and south. Asymmetry in Ne exists at altitudes near and above the ionospheric peak, especially in the topside ionosphere (e.g., 400 km), indicating that the asymmetry is caused mainly by neutral wind. Also, in all longitudes (75°E, 75°W, and 45°W) the denser ionosphere is in the hemisphere of equatorward wind, compare Figs. 4–6 with the winds in Fig. 3.

Figs. 4–6 also show that at 75°E and 75°W the ionospheric asymmetry is strong, and the denser ionosphere is in opposite hemispheres (south at 75°E and north at 75°W) where neutral winds are equatorward (compare with the winds in Fig. 3). Also, at 45°W the ionosphere has comparatively weak asymmetry though similar to that at 75°W. These results seem to indicate that the north–south differences in the neutral wind velocity arising from the displacement of the equators is more effective in producing the north–south asymmetry in the ionosphere than that arising from declination angle; discussed in Section 5.

3.2. Electric field effect

As mentioned above the model results in Section 3.1 were obtained using the same electric field (blue, Fig. 2) in all three longitudes. To check the effect of the differences in the electric fields, the model calculations in all three longitudes are repeated using the respective **E** × **B** drift velocities (Fig. 2). The resulting model TEC at 13 LT are shown by the dashed curves in Fig. 6 (red 75°E, blue 75°W, and green 45°W); the blue solid and dashed curves (75°W) coincide as they are obtained using the same **E** × **B** drift. A comparison of the solid and dashed curves (Fig. 6) shows no significant differences, which seems to indicate that the longitude variation of the east–west electric field has only a small effect on the longitude variation of the north–south asymmetry of the ionosphere compared to the longitude variation of neutral wind; discussed in Section 5.

4. FORMOSAT-3/COSMIC data

The FORMOSAT-3/COSMIC satellite measures the electron density Ne up to 800 km height on a global scale using radio occultation technique (Lin et al., 2007; Liu et al., 2010b). However, the density in the bottomside ionosphere (below about 250 km) may not be reliable due to the limitations of the technique (Liu et al., 2010b; and references therein). The COSMIC Ne data have been used to study several aspects of the global ionosphere at the long deep solar minimum, and revealed some new aspects such as plasma caves in the bottomside low latitude ionosphere (Liu et al., 2010a), longitude structure of F_3 layer (Zhao et al., 2011), and reversal of the hemisphere of high electron density from winter hemisphere to summer hemisphere (or disappearance of winter anomaly) after noon (e.g., Lin et al., 2007; Tulasi Ram et al., 2009; Liu et al., 2010b; Balan et al., 2012).

In this section, we show the north–south asymmetry in the mean COSMIC electron density at around diurnal maximum (12:30–13:30 LT) under magnetically quiet ($Ap < 15$) equinoctial conditions in 2008–2010 in different longitudes. Fig. 7 shows the altitude-latitude plots of the data in the longitude sectors 60°E–120°E (panel a) and 60°W–120°W (panel b). Fig. 8 is for the longitude sector 15°W–75°W (panel a), with panels b and c showing the data in the sub-longitude sectors 45°W–75°W and 45°W–15°W. A common color scale is used in all figures for easy comparison. The data distribution is found to be nearly uniform in latitude in all longitudes.

As shown by the COSMIC data, the north–south ionospheric asymmetry is (1) significant in the longitude sectors 60°E–120°E and 60°W–120°W (Fig. 8) of large displacement of the equators with small declination angle, and (2) weak in the longitude sector 15°W–75°W (Fig. 8, panel a) of large declination angle with small displacement of the equators; (3) the denser ionosphere in the 60°E–120°E and 60°W–120°W longitudes is in opposite hemispheres (Fig. 8, panels a and b) where the geomagnetic equator is displaced from geographic equator; (4) the asymmetries in the sub-longitude sectors 15°W–45°W and 45°W–75°W of large declination angle with small and opposite displacement of the equators (Fig. 8, panels b and c) is stronger than that

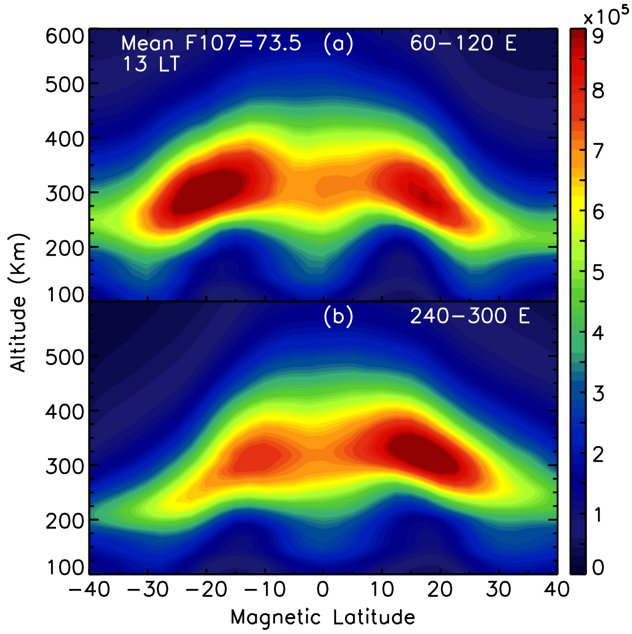

Fig. 7. Altitude–latitude plots of mean COSMIC electron density at 13 LT (12:30–13:30 LT) at magnetically quiet (Ap < 15) equinoctial conditions (March–April and September–October) in 2008–2010 in longitude sectors (a) 60°E–120°E and (b) 240°E–300°E (60°W–120°W); positive latitude is north.

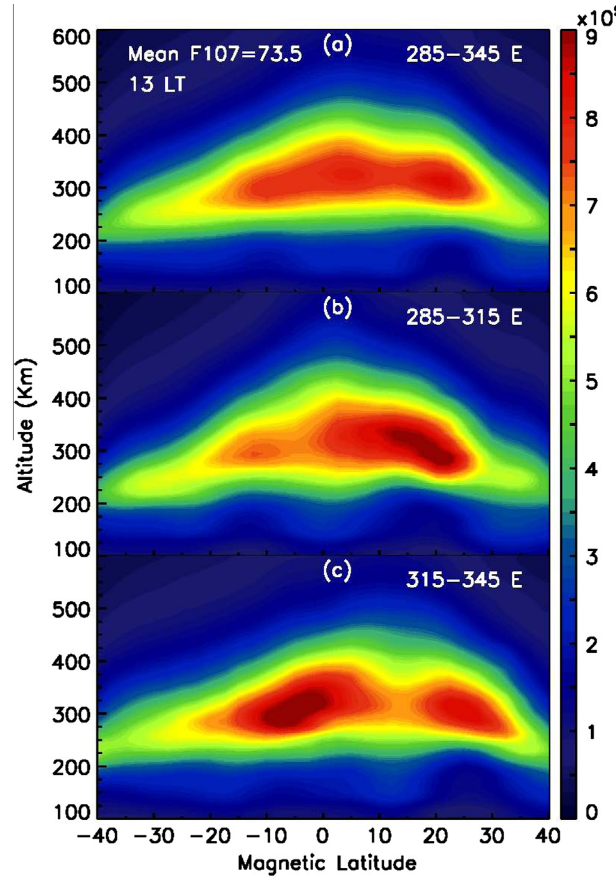

Fig. 8. Same as Fig. 7 but in longitude sectors (a) 285°E–345°E (15°W–75°W), (b) 285°E–315°E (45°W–75°W) and (c) 315°E–345°E (15°W–45°W).

in the combined longitude sector 15°W–75°W (Fig. 8, panel a); and (5) the denser ionosphere in the two sub-longitude sectors 45°W–75°W and 45°W–15°W is also in opposite hemispheres where geomagnetic equator is displaced. These observed features of the north–south ionospheric asymmetry are in good qualitative agreement with the model predictions (Figs. 4–8), and indicate that displacement of the geomagnetic equator from geographic equator is most effective in producing the north–south asymmetry than magnetic declination angle, discussed below.

5. Discussion

The main points that came out from the observations and modeling of the north–south asymmetry in the ionospheric F region at around diurnal maximum (13 LT) at equinoxes at the long deep solar minimum are discussed.

(1) The ionospheric asymmetry is such that the ionosphere is dense in one hermisphere and weak in the opposite hemisphere. This, as mentioned in Section 1, is mainly due to the north–south difference in the effective magnetic meridional neutral wind velocity U (Eq. (1)). The ionosphere becomes dense in the hemisphere of equatorward (or less poleward) wind and weak in the opposite hemisphere of poleward wind. The equatorward wind (i) raises (and supports) the ionosphere to high altitudes of reduced chemical loss by an altitude proportional to UcosIsinI with I being dip angle, and (ii) opposes (or reduces) the downward field-aligned flow of plasma by UcosI (Balan et al., 2010). The processes (i) and (ii) together increase Ne, Nmax and TEC in the hemisphere of equatorward wind. At the same time the poleward wind in the opposite hemisphere lowers the ionosphere in altitude and also accelerates the downward field-aligned flow down to low altitudes of heavier chemical loss. That causes the north–south ionospheric asymmetry.

(2) The north–south asymmetry is strong in longitudes of large displacement of the equators with small declination angle, and weak in longitudes of large declination angle with small displacement of the equators (e.g., Figs. 4–8). This is because the displacement of the equators is more effective in changing the wind velocity U than is the declination angle. This can be understood from the values of U (Fig. 3). For example, at 75°W (at 13 LT and 16°S magnetic latitude) where displacement is large (∼12°) and declination is small (−1.87°) $U = -27.94\ m\ s^{-1}$ (panel b). On the other hand at 45°W (at 13 LT and 16°S magnetic latitude) where the displacement is small (0°) and declination is large (−18.83°) $U = -16.10\ m\ s^{-1}$. In other words, large displacement of the equators and

large declination angle provide large and small values of U, respectively, and hence cause strong and weak north–south asymmetry in the ionosphere.

(3) Though the asymmetry is strong in 75°E and 75°W the denser ionosphere is in opposite hemispheres (e.g., Figs. 4–8). This is because in these longitudes the displacements of the geomagnetic equator is large (~7° and −12°) but in opposite hemispheres (Fig. 1).

(4) The points (1), (2), and (3) can be discussed further with the equatorial plasma fountain. Fig. 9 shows the model plasma fountain at 12 LT at 75°W; the fountain is shown for only one longitude, for simplicity. The plasma flux (product of density and velocity, Fig. 9) is strong in the southern hemisphere of poleward wind but the ionosphere is strong (in Nmax and TEC) in the opposite hemisphere of equatorward wind (e.g., Figs. 4–8). This is because in the hemisphere of poleward wind the ionosphere lowers in altitude and downward field-aligned plasma flow gets accelerated down to low altitudes of heavy chemical loss, which reduce Nmax and TEC. At the same time, in the opposite hemisphere of equatorward wind the ionosphere gains ionization by rising to high altitudes of reduced chemical loss and by reducing the downward field-aligned flow.

The chemical (or composition change) effect of the wind can increase the O/N_2 ratio in the hemisphere of poleward wind and decrease the ratio in the opposite hemisphere of equatorward wind. However, the composition (O/N_2) does not seem to have any significant north–south difference as understood from the nearly equal Ne values in the bottomside ionosphere (~200 km, Fig. 5). It may also be recalled that the north–south ionospheric asymmetry occurs near the ionospheric peak and above (Fig. 5) where the mechanical (or dynamical) effects of the wind dominate over its chemical effect.

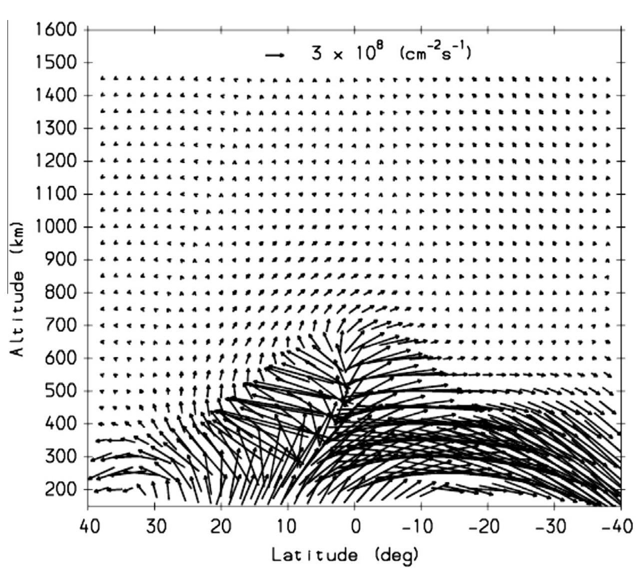

Fig. 9. Model plasma fountain at 12 LT at March equinox (day 80) for Ap = 4 and F10.7 = 68 in 75°W; minimum vector length corresponds to plasma flux < 2×10^5 cm^{-2} s^{-1}; latitude is magnetic and positive latitude is north.

(5) The longitude variation of the electric field (or upward **E** × **B** drift) has only small effect compared to that of neutral wind on the longitude variation of the ionospheric asymmetry (e.g., Fig. 6). This is because of the difference in the importance of the **E** × **B** drift and neutral wind in determining the strength of the low latitude ionosphere. The **E** × **B** drift controls the strength of the ionosphere only at around the equator (within about ±10° magnetic latitudes) in all longitudes, where ionosphere is generally weak due to the upward drift removing the ionization to higher altitude-latitude regions. At higher latitudes, neutral wind takes control and makes the ionosphere stronger especially when the wind is equatorward as discussed in point (1) above.

It may be mentioned that the effects of the displacement of the equators and declination angle are same for all levels of solar activity since the displacement and declination are independent of solar activity. However, the wind velocity could be faster at the long deep solar minimum compared to higher levels of solar activity due to reduced ion-drag.

6. Conclusions

Longitude variation of the north–south asymmetry of the ionosphere at around diurnal maximum at equinoxes at low latitudes (±30° magnetic) is investigated using SUPIM and COSMIC electron density data measured at the long deep solar minimum (2008–2010). The asymmetry is found to be strong in longitudes (e.g., around 75°E and 75°W) of large displacement of geomagnetic equator from geographic equator than in longitudes (e.g., around 45°W) of large declination angle. This seems to be because it is the displacement more than the declination angle that produces large north–south difference in the magnetic meridional neutral wind velocity, which is the main cause of the ionospheric asymmetry. For the strong control of the neutral wind, east–west electric field has only a weak effect on the longitude variation of the ionospheric asymmetry. The conclusions seem valid for all levels of solar activity since the displacement of the equators and declination angle are independent of solar activity.

Acknowledgments

We thank National Science Council (NSC) of Taiwan for the grants NSC98-2111-M-008-008-MY3 and NSC100-2811-M-008-034 under which this work is carried out.

References

Abdu, M.A. Equatorial spread F development and quiet time variability under solar minimum conditions. Indian J. Radio Space Phys. 41, 168–183, 2012.

Bailey, G.J., Balan, N., 1996. A low latitude ionosphere–plasmasphere model. In: Schunk, R.W. (Ed.), STEP Hand Book of ionospheric models, Utah State University, Logan, UT 84322–4405,p. 173.

Balan, N., Bailey, G.J., Moffett, R.J., Su, Y.Z., Titheridge, J.E. Modelling studies of conjugate-hemisphere differences in ionospheric ionization at equatorial anomaly latitudes. J. Atmos. Terr. Phys. 57, 279, 1995.

Balan, N., Bailey, G.J., Abdu, M.A., Oyama, K.I., Richards, P.G., Macdougall, , Batista, I.S. Equatorial plasma fountain and its effects over three locations: evidence for an additional layer – F3 layer. J. Geophys. Res. 102, 2047, 1997.

Balan, N., Shiokawa, K., Otsuka, Y., Kikuchi, T., Vijaya Lekshmi, D., Kawamura, S., Yamamoto, M., Bailey, G.J. A Physical mechanism of positive ionospheric storms at low and mid latitudes through observations and modeling. J. Geophy. Res. 115, A02304, http://dx.doi.org/10.1029/2009JA014515, 2010.

Balan, N., Chen, C.Y., Liu, J.Y., Bailey, G.J. Behavior of the low latitude ionosphere-thermosphere system at long deep solar minimum. Indian J. Radio Space Phys. 41, 89–97, 2012.

Girish, T.E., Gopkumar, G. Secular changes in the solar terrestrial conditions observed during sunspot minima: some implications for the earth's ionosphere. Indian J. Radio Space Phys. 41, 83–88, 2012.

Goncharenko, L.P., Chau, J.L., Liu, H.L., Coster, A.J. Unexpected connection between the stratosphere and ionosphere. Geophys. Res. Lett. 37, L10101, http://dx.doi.org/10.1029/2010GL043125, 2010.

Hedin, A.E. MSIS-86 thermospheric model. J. Geophys. Res. 92, 4649, 1987.

Hedin, A.E. et al. Revised global model of thermosphere winds using satellite and ground-based observations. J. Geophys. Res. 96, 7657, 1991.

Heelis, R.A., Coley, W.R., Burrell, A.G., Hairston, M.R., Earle, G.D., Perdue, M.D., Power, R.A., Harmon, L.L., Holt, B.J., Lippincott, C.R. Behavior of the O^+/H^+ transition height during the extreme solar minimum of 2008. Geophys. Res. Lett. 36, L00C03, http://dx.doi.org/10.1029/2009GL038652, 2008.

Lin, C.H., Liu, J.Y., Fang, T.W., Chang, P.Y., Rsai, H.F., Chen, C.H., Hsiao, C.C. Motions of the equatorial ionization anomaly crests imaged by FORMOSAT-3/COSMIC. Geophys. Res. Lett. 34, L19101, http://dx.doi.org/10.1029/2007GL030741, 2007.

Liu, J.Y., Lin, C.Y., Lin, C.H., Tsai, H.F., Solomon, S.C., Sun, Y.Y., Lee, I.T., Schreiner, W.S., Kuo, Y.H. Artificial plasma cave in the low-latitude ionosphere results from the radio occultation inversion of the FORMOSAT-3/COSMIC. J. Geophy. Res. 115, A07319, http://dx.doi.org/10.1029/2009JA015079, 2010a.

Liu, L., He, M., Yue, X., Ning, B., Wan, W. Ionosphere around equinoxes during low solar activity. J. Geophys. Res. 115, A09307, http://dx.doi.org/10.1029/2010JA015318, 2010b.

Luhr, H., Xiong, C. IRI-2007 model overestimates electron density during the 23/24 solar minimum. Geophys. Res. Lett. 37, L23101, http://dx.doi.org/10.1029/2010GL045430, 2010.

Mehmet, A. North-south asymmetry in the ionospheric equatorial anomaly in the African and the West Asian regions produced by asymmetrical thermospheric winds. J. Atmos. Terr. Phys. 50, 623, 1988.

Russell, C.T., Luhmann, J.G., Jian, L.K. How unprecedented a solar minimum? Rev. Geophys. 48, RG2004, http://dx.doi.org/10.1029/2009RG000316, 2010.

Su, Y.Z., Bailey, G.J., Oyama, K.I., Balan, N. A modelling study of the longitudinal variations in the north–south asymmetries of the ionospheric equatorial anomaly. J. Atmos. Terr. Phys. 59, 1299, 1997.

Stoneback, R.A., Heelis, R.A., Burrell, A.G., Coley, W.R., Fejer, G.G., Pacheco, E. Observations of quiet time vertical ion drift in the equatorial ionosphere during the solar minimum period of 2009. J. Geophys. Res. 116, A11312, http://dx.doi.org/10.1029/2011JA016715, 2011.

Tobiska, W.K. Revised solar extreme untraviolet flux model. J. Atmos. Terr. Phys. 53, 1005, 1991.

Tulasi Ram, S., Su, S.-Y., Liu, C.H. FORMOSAT-3/COSMIC observations of seasonal and longitudinal variations of equatorial anomaly and its inter-hemispheric asymmetry during the solar minimum period. J. Geophys. Res. 114, A06311, http://dx.doi.org/10.1029/2008JA013880, 2009.

Zhang, S.-R., Foster, J.C., Holt, J.M., Erickson, P.J., Coster A.J., Magnetic declination and zonal wind effects on longitudinal differences of ionospheric electron density at mid latitudes, J. Geophys. Res. 117, A08329, http://dx.doi.org/10.1029/2012JA017954, 2012.

Zhao, B., Wan, W., Yue, X., Liu, L., Ren, Z., He, M., Liu, J. Global characteristics of occurrence of an additional layer in the ionosphere observed by COSMIC/FORMOST-3. Geophys. Res. Lett. 38, http://dx.doi.org/10.1029/2010GL045744, 2011.